

Controllable Synthesis of ZnO Nanorod-nanosheets Hierarchical Nanostructure on a Stainless Steel Mesh Via A Facile Hydrothermal Growth

Shibu ZHU^{1,a}, Jingpeng ZHAO¹, Xiaohu ZHANG¹, Hong CUI¹ and Zuowan ZHOU²

¹ Xi'an Aerospace Composites Research Institute, Xi'an, 710025, P R China

² Key Laboratory of Advanced Technologies of Materials (Ministry of Education), School of Materials Science and Engineering, Southwest Jiaotong University, Chengdu, 610031, P R China

^a 19860917zsb@163.com

Abstract. ZnO nanorods-nanosheets (NR-NS) hierarchical nanostructure consisted of long nanorod and thin nanosheet branches have been built on a stainless steel mesh via a two-step hydrothermal growth process. The related structures and morphologies of the as-prepared products were characterized by X-ray diffraction (XRD) and field emission scanning electron microscopy (FE-SEM). The XRD results confirmed that the obtained samples were wurtzite hexagonal structured ZnO. The FE-SEM observations showed that the smooth surfaces of nanorods were covered by nanosheets, resulting in the enhancement of internal surface area. It was found that trisodium citrate played a crucial role in the formation of ZnO NR-NS hierarchical nanostructures, and accordingly, the rational growth mechanism was suggested.

Keywords: Stainless steel mesh; ZnO NR-NS hierarchical nanostructure; Hydrothermal method; Trisodium citrate

1 Introduction

To date, due to the increasing demand for energy and consumption of fossil fuels, finding new energy sources has steadily grown. Solar energy is considered as one of most promising candidates of all alternative energy. Much attention has been paid to dye-sensitized solar cells (DSSCs) owing to their low cost, simplified manufacturing process and possible of large-scale production for next generation solar cells ^[1, 2]. Recently, ZnO with one dimensional (1-D) structures, such as nanowires^[3], nanograss ^[4] and nanotubes ^[5], have been built for improving conversion efficiency of DSSCs because of their superior electron mobility. However, this kind of DSSCs is commonly based on a rigid FTO or ITO glass substrate, which restricts its adaptability during transportation, installation and flexible application. Flexible DSSCs is a new research field displaying potential application in powering mobile electronic products. Until now, two main kinds of flexible substrates are used for DSSCs, transparent polymer substrates and metal sheets ^[6, 7]. Compared to plastic

and polymer substrates, metal sheet can withstand a high-temperature sintering process and possesses high crystallization of the semiconductor. Recently, stainless steel mesh substrate received much attention^[8]. The challenge in fabricating stainless steel mesh based flexible DSSCs lies in the successful construction of a well-defined semiconductor oxide on round-like wires to achieve desirable performances. So, it is well worth developing a facile approach to construct nanostructure on stainless steel mesh.

On the other hand, wastewater emissions from the textile industry contain large amounts of dyes, which are considered a major threat to the adjacent ecosystem due to their non-biodegradability, toxicity, and potential carcinogenicity^[9]. Dye removal by photoinduced decomposition of pollutants on photocatalysts has been widely researched^[10]. ZnO is also considered as an effective photocatalyst for degrading contaminants^[11]. However, most photocatalysts that were studied previously were mobile-type, and only a few immobilized photocatalysts have been reported although they have notable advantages over mobile-type catalysts from a practical perspective. Meanwhile, immobilized photocatalysts showed poor performance due to their closed surface, leading to inefficient mass transference. Thus, ZnO hierarchical nanostructures built on the stainless steel mesh substrate might present an extensive surface area for photocatalysis.

Herein, we demonstrated a facile two-step hydrothermal procedure of constructing ZnO nanorods-nanosheets (NR-NS) hierarchical nanostructures on a stainless steel mesh substrate. 1-D ZnO nanorods perpendicular to the cylindrical metal micro-wires were synthesized and served as a backbone for the second hydrothermal growth of ZnO nanosheets. The stainless steel mesh supported ZnO NR-NS hierarchical nanostructure possessed large surface area, and it was expected to use as a photoanode for DSSCs or immobilized photocatalysts with the enhancement of related performance.

2 Experiment

2.1 Synthesis of ZnO nanorod-nanosheet hierarchical nanostructure

Zinc nitrate hydrate ($\text{Zn}(\text{NO}_3)_2 \cdot 6\text{H}_2\text{O}$, 99%, Aladdin), zinc acetate ($\text{Zn}(\text{CH}_3\text{COO})_2 \cdot 2\text{H}_2\text{O}$, 99%, Aladdin), hexamethylenetetramine (HMTA, 99%, Aladdin), trisodium citrate ($\text{C}_6\text{H}_5\text{Na}_3 \cdot 2\text{H}_2\text{O}$, AR, Aladdin) and polyethylenimine (PEI, $M_w=800$, Sigma-Aldrich) were used as received without further purification. The stainless steel mesh (Jinhongyuan Metal Mesh Co., China) was cleaned ultrasonically in acetone, ethanol and distilled water for 15 min, respectively. The growth procedure of the ZnO NR-NS hierarchical nanostructures on a stainless steel mesh is schematically illustrated in Figure 1. The first hydrothermal growth of ZnO nanorods was as similar as our previous work^[12]. In a typical process, a ZnO-seeded stainless steel mesh substrate was vertically immersed into the solution containing 25 mM $\text{Zn}(\text{NO}_3)_2$, 25 mM HMTA, and 7 mM PEI, and the hydrothermal reaction was carried out in a sealed vessel at 92°C for 20 h. The growth solutions were refreshed every 4 h during the reaction period. For the subsequent growth procedure of ZnO hierarchical nanostructure, the stainless steel mesh substrate coated with ZnO nanorods was transferred into a vessel containing 10 mM $\text{Zn}(\text{NO}_3)_2$, 10 mM HMTA and 1 mM $\text{C}_6\text{H}_5\text{Na}_3$ aqueous solution, and the reaction was carried out at 70°C for 5 h, resulting in ZnO NR-NS hierarchical nanostructure. Then, the obtained samples were rinsed with absolute ethanol and distilled water, respectively, and finally dried in air for next characterization.

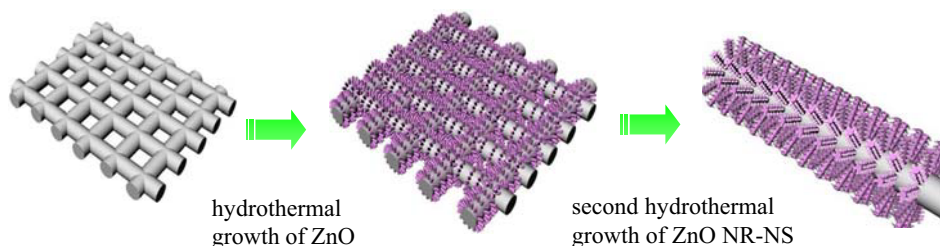


Figure 1 Schematic growth procedure of the ZnO NrR-NS hierarchical nanostructure on a stainless steel mesh

2.2 Characterization

X-ray diffraction measurements were performed through a Philips X'Pert PRO X-ray diffractometer (XRD, The Netherlands) with a $\text{CuK}\alpha$ radiation to verify the phase and crystal structure of the ZnO films. The morphologies of ZnO nanorods and ZnO NR-NS hierarchical nanostructure films were characterized by field emission scanning electron microscope (FE-SEM, JSM-7001F, JEOL).

3 Results and Discussion

The ZnO NR-NS hierarchical nanostructure on the stainless steel mesh was synthesized by means of a two-step hydrothermal growth. Firstly, ZnO nanorods array was prepared on a stainless steel mesh by hydrothermal process. Secondly, the second-step hydrothermal reaction of ZnO nanorods was carried out in the solution containing $\text{Zn}(\text{NO}_3)_2$, HMTA and $\text{C}_6\text{H}_5\text{Na}_3\cdot 2\text{H}_2\text{O}$, resulting in the formation of ZnO NR-NS hierarchical nanostructure. The crystal structures of the stainless steel mesh substrate and as-synthesized samples were characterized by X-ray diffraction (XRD), as shown in Figure 2. The as-prepared sample after the hydrothermal reaction can be indexed as the hexagonal wurtzite-phase, corresponding to (100), (002), (101), (102), (110), (103) and (112) planes of ZnO (JCPDS Card No. 00-036-1451). At the same time, it is obvious that the diffraction peaks at $2\theta=43.47^\circ$, 50.67° and 74.68° are well assigned to (111), (200) and (220) planes of stainless steel mesh substrate, according to the JCPDS Card No. 00-023-0298, as marked in Figure 2c, respectively. No characteristic peaks arising from reactants or intermediate products are detected, implying the high purity of the prepared ZnO nanostructure. The diffraction peak intensity corresponded to the ZnO (002) plane, centered at about 34.34° , surpasses others of ZnO diffraction peaks, indicating that a high degree of orientation along [001] direction that was perpendicular to the stainless steel mesh substrates.

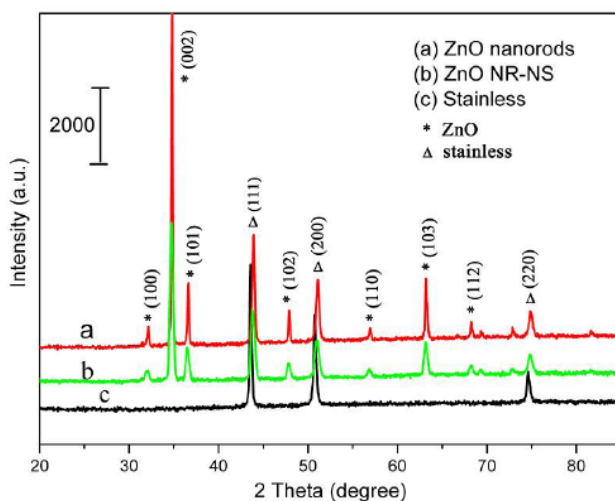


Figure 2 XRD profiles of a stainless steel mesh substrate and as-obtained sample by hydrothermal growth

The microstructure of stainless steel mesh substrate was characterized by field emission scanning electron microscope (FE-SEM). Figure 3a and b show the top and cross-section views SEM images of a stainless steel mesh substrate. It clearly showed that the substrate was made of the metal round wires with a diameter of about 30 μm and quite a smooth surface. The area of the pores was *ca.* 35 \times 35 μm^2 . The porous structures of the stainless steel mesh were in favor of ZnO growth along with radical direction of a metal wire. Thus, after a ZnO seed layer prepared on the stainless steel mesh by dip-coating and pyrolysis, ZnO nanostructure could be webbed with round-shaped wires.

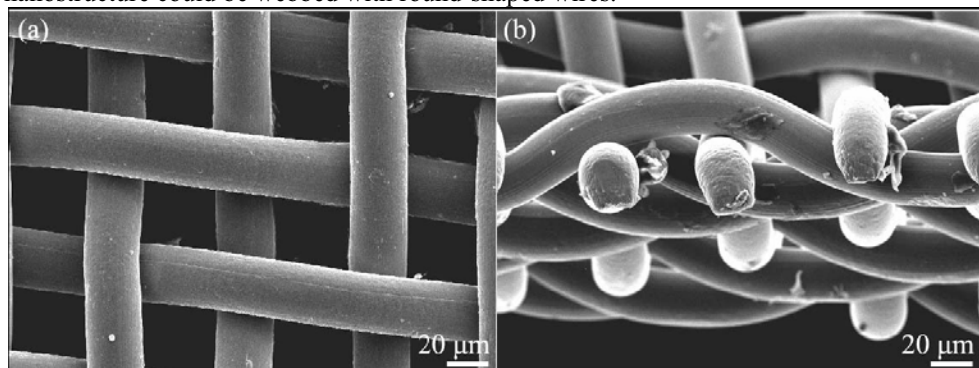


Figure 3 Top view (a) and cross-section (b) SEM images of stainless steel substrate

The color of the stainless steel mesh became white instead of metal luster after the hydrothermal growth, indicating a successful coating with ZnO nanostructure. The microstructure of obtained samples was displayed in Figure 4. It was found that the diameter of round-like wire increased to 38 μm , indicating that ZnO nanorod arrays was uniformly fabricated on the mesh substrate, which was webbed with round-shaped wires (Figure 4a). It was speculated that the length of ZnO nanorods was 4 μm . The high-magnification scanning electron microscope image conformed that ZnO nanorods formed a dense vertically-aligned array in which the diameter of a single nanorod was about 100-150 nm (Figure 4b). Further hydrothermal reaction of ZnO nanorods/stainless steel mesh in the solution containing

$\text{Zn}(\text{NO}_3)_2$, HMTA and $\text{C}_6\text{H}_5\text{Na}_3 \cdot 2\text{H}_2\text{O}$ led to formation of ZnO NR-NS hierarchical nanostructure consisted of long nanorod backbone and thin nanosheets, as shown in Figure 4c and d. The length of ZnO NR-NS hierarchical nanostructure was also about $4 \mu\text{m}$. However, it was clear that the smooth surfaces of ZnO nanorods were surrounded by the thin nanosheets, forming the rough “shell” out of the ZnO nanorods, and the average diameter of the ZnO NR-NS hierarchical nanostructure was significantly increased. It had been proven that the smooth surfaces of nanorods covered by nanosheets could result in the enhancement of internal surface area^[13, 14]. The flexible ZnO NR-NS hierarchical nanostructures film might be applied to solar cells and photocatalytic areas.

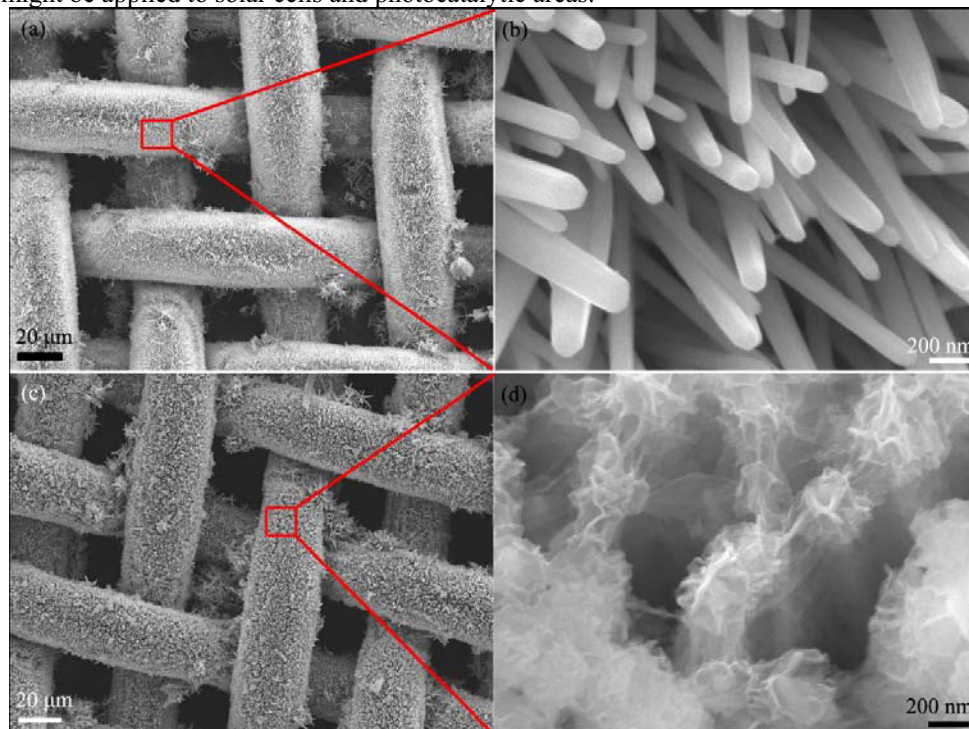


Figure 4 Top-view SEM images of ZnO nanorods (a, b) and ZnO NR-NS hierarchical nanostructure (c, d) on a stainless steel mesh substrate

The ZnO NR-NS hierarchical nanostructure was formed during the second hydrothermal reaction. Compared to the first hydrothermal growth, trisodium citrate was taken place of PEI in the reaction aqueous solution. So, trisodium citrate played an important role in the formation of the nanosheet on the surface of the ZnO nanorods. As well known, rod-like ZnO would be received if no citrate anion was added in the reaction solution, due to the higher surface energy of (001) plane and resulting in a faster growth rate along [001] direction^[15]. However, in the presence of citrate anion, the citrate ion can adsorb onto the positive charged Zn^{2+} terminated (001) polar plane due to the Coulombic force^[16]. The adsorption effectively slowed down the crystal growth along the [001] direction. At the early growth phase of the second hydrothermal reaction, lots of ZnO nanoparticles were formed on the surface of ZnO nanorods. As the reaction continued, ZnO nanoparticles underwent oriented attachment sideways to formation of nanosheets on the surface of ZnO nanorods. Based on our results, it was speculated that ZnO NR-NS hierarchical nanostructures prepared by a two-step citrate assisted hydrothermal procedure could be applied to other substrates for building ZnO hierarchical nanostructures.

4 Conclusion

In summary, a facile two-step hydrothermal process was developed to prepare ZnO NR-NS hierarchical nanostructures containing long ZnO nanorods backbones and thin ZnO nanosheet branches on the stainless steel mesh. Based on the XRD results, wurtzite hexagonal structured ZnO was obtained. It was clear that nanosheets were uniformly covered on the surface of ZnO nanorods, resulting in enhancement of internal surface area. Meanwhile, the mechanism of ZnO NR-NS hierarchical nanostructures on the stainless steel mesh was discussed. We expect that this useful and simple approach to prepare ZnO hierarchical nanostructure will offer many promising applications in the future.

References

1. B. O'regan, M. Grätzel, A low-cost, high-efficiency solar cell based on dye-sensitized colloidal TiO₂ films, *Nature* 353 (1991) 737-740.
2. A. Yella, H.W. Lee, H.N. Tsao, C. Yi, A.K. Chandiran, M.K. Nazeeruddin, E.W. G. Diau, C. Y. Yeh, S.M. Zakeeruddin, M. Grätzel, Porphyrin-sensitized solar cells with cobalt (II/III)-based redox electrolyte exceed 12 percent efficiency, *Science* 334 (2011) 629-634.
3. M. Law, L. Greene, J. Johnson, R. Saykally, P. Yang, Nanowire dye-sensitized solar cells, *Nat. Mater.* 4 (2005) 455-459.
4. S. B. Zhu, W. Wei, X. N. Chen, M. Jiang, Z. W. Zhou, Hybrid structure of polyaniline/ZnO nanograss and its application in dye-sensitized solar cell with performance improvement, *J. Solid State Chem.* 190 (2012) 174-179.
5. A. Martinson, J. Elam, J. Hupp, M. Pellin, ZnO nanotube based dye-sensitized solar cells, *Nano Lett.* 7 (2007) 2183-2187.
6. L. Y. Lin, M. H. Yeh, C. P. Lee, C. Y. Chou, R. Vittal, K. C. Ho, Enhanced performance of a flexible dye-sensitized solar cell with a composite semiconductor film of ZnO nanorods and ZnO nanoparticles, *Electrochim. Acta* 62 (2012) 341-347.
7. H. W. Chen, C. Y. Lin, Y. H. Lai, J. G. Chen, C. C. Wang, C. W. Hu, C. Y. Hsu, R. Vittal, K. C. Ho, Electrophoretic deposition of ZnO film and its compression for a plastic based flexible dye-sensitized solar cell, *J. Power Sources* 196 (2011) 4859-4864.
8. H. Dai, Y. Zhou, Q. Liu, Z. D. Li, C. X. Bao, T. Yu, Z. G. Zhou, Controllable growth of dendritic ZnO nanowire arrays on a stainless steel mesh towards the fabrication of large area, flexible dye-sensitized solar cells. *Nanoscale* 4 (2012) 5454-5460.
9. H. Tada, M. Kubo, Y. Inubushic, S. Itob, N=N bond cleavage of azobenzene through Pt/TiO₂ photocatalytic reduction *Chem. Commun.* (2000) 977-978.
10. Z. Liu, X. Zhang, S. Nishimoto, M. Jin, D. A. Tryk, T. Murakami, A. Fujishima, Highly ordered TiO₂ nanotube arrays with controllable length for photoelectrocatalytic degradation of phenol. *J. Phys. Chem. C* 112(2008) 253-259.
11. X. L. Xu, X. Duan, Z.G. Yi, Z.W. Zhou, X.M. Fan, Y. Wang, Photocatalytic production of superoxide ion in the aqueous suspensions of two kinds of ZnO under simulated solar light. *Catal. Comm.* 12 (2010) 169-172.
12. S. B. Zhu, X. N. Chen, F. B. Zuo, M. Jiang, Z. W. Zhou, D. Hui, Controllable synthesis of ZnO nanograss with different morphologies and enhanced performance in dye-sensitized solar cells, *J. Solid State Chem.* 197 (2013) 69-74.
13. S. B. Zhu, L. M. Shan, X. N. Chen, L. He, J. J. Chen, M. Jiang, X. L. Xie, Z. W. Zhou,

- Hierarchical ZnO architectures consisting of nanorod and nanosheet via a solution route for photovoltaic enhancement in dye-sensitized solar cells, *RSC Adv.* 3 (2013) 2910-2916.
14. S. B. Zhu, L. M. Shan, X. Tian, X. Y. Zheng, D. Sun, X. B. Liu, L. Wang, Z. W. Zhou, Hydrothermal synthesis of oriented ZnO nanorod-nanosheets hierarchical architecture on zinc foil as flexible photoanodes for dye-sensitized solar cells, *Ceram. Int.* 40 (2014) 11663-11670.
 15. B. Weintraub, Z. Zhou, Y. Li, Y. Deng, Solution synthesis of one-dimensional ZnO nanomaterials and their applications. *Nanoscale* 2 (2010) 1573-1587.
 16. J. A. Parkinson, H. Sun, New approach to the solution chemistry of bismuth citrate antiulcer complexes. *Chem. Commun.* (1998) 881-882.